



Fatigue performance of RC beams strengthened with self-prestressed iron-based shape memory alloys

Hothifa Rojob, Raafat El-Hacha*

University of Calgary, 2500 University Drive NW, Calgary, AB T2N 1N4, Canada

ARTICLE INFO

Keywords:

Fatigue loading
Shape memory alloys
Self-prestressing
Near-surface mounted

ABSTRACT

The behavior of RC beams strengthened with self-prestressed NSM Iron-Based Shape Memory Alloy (Fe-SMA) bars under fatigue loading is experimentally investigated. Four beams divided into two sets are tested; the first set of beams is exposed to 6 million cycles of fatigue loading at different loading limits, while no fatigue loading is applied to the second set. Each set contains one control beam and one strengthened beam. The results of the first static load cycle indicates that strengthening with NSM Fe-SMA bars significantly improves the performance of the RC beams under service load conditions. During fatigue loading, the beam strengthened with NSM Fe-SMA performs much better than the control beam at relatively low levels of fatigue loading (when the upper and lower limit of the fatigue loading induces $0.29f_y$ and $0.53f_y$ stress in the tension steel of the control beam, respectively). The stiffness degradation of the strengthened beam stabilizes after two million loading cycles. However, higher load limits cause continued degradation in the bond between the Fe-SMA bar and the grouting material. This degradation causes higher stress levels at the anchors, which consequently provokes the rupture of the Fe-SMA bar at the anchors' location after 5.5 million loading cycles.

1. Introduction

Many countries suffer from severe deterioration in bridges due to ageing and significant increase in the load demand. In the United States, 200 million trips are taken daily across deficient bridges [1], and the estimated replacement cost of those bridges is about \$51.8 billion (US dollars)[2]. In Canada, 60% of the bridges in the national highway system are more than 30 years old, and 15% of them are more than 50 years old, and many of them require major rehabilitation [3]. In light of the mentioned facts, a practical and efficient structural rehabilitation technique is essential.

The use of Fibre Reinforced Polymers (FRP) in the rehabilitation and strengthening of Reinforced Concrete (RC) structures has been widely adopted by researchers and implemented in design codes and standards, as well as in several filed applications. One of the most efficient techniques in FRP strengthening is the Near-Surface Mounted (NSM) system, where the FRP material is embedded in a pre-cut groove along the tension side of the RC beam then filled with epoxy adhesive; this technique ensures a better bond with the grouting material and protection for the FRP material [4]. Strengthening using FRP can be either passive, where no prestressing force is applied to the strengthening material, or active in the case of prestressed FRP. In passive strengthening, the FRP mainly contributes to the flexural performance of the RC

beam at ultimate load conditions with minimal contribution under service load conditions [5,6]. Whereas, in the case of the active strengthening, the performance of the RC beam is enhanced at service conditions due to the presence of the prestressing force, which counteracts the applied loads, and consequently, reduces cracking and deflection [5,6]. There are several techniques to apply the prestressing force to the FRP material, such as using external frames [6] or by prestressing against the beam itself [4,7–9]. In many cases, the application of the prestressing force to the FRP material is a sophisticated and too laborious process, and the procedure is case-dependent due to the need for special anchorages and jacking tools.

Recent studies showed the effectiveness of the self-prestressing system using NSM Fe-SMA [10,11] and using Fe-SMA bars embedded in shotcrete layer [12]. The application of the prestressing force did not require any jacking tools, where the prestressing force was developed through heating. Additionally, due to the yielding nature of the Fe-SMA material, the behavior of the beams strengthened with the Fe-SMA material, which failed in a ductile manner by crushing of concrete after yielding of the reinforcements and the Fe-SMA material, was similar to the under-reinforced beam [13].

Further, the Fe-SMA material is relatively inexpensive compared to the commonly used Nickel Titanium SMA (NiTi-SMA). Also, the availability of the regular steel bars' mass production facilities is expected to

* Corresponding author.

E-mail addresses: hrojob@ucalgary.ca (H. Rojob), relhacha@ucalgary.ca (R. El-Hacha).

Nomenclature

A	beam cross-sectional area
A_f	austenite finish temperature
A_s	austenite start temperature
e	eccentricity of the Fe-SMA bar with respect to the centroid of the beam cross-section
E_c	concrete modulus of elasticity
F	the prestressing force developed in the Fe-SMA bars
f_c	concrete compressive strength
f_y	steel reinforcements yield strength
I_g	area moment of inertia

P_{cr}	cracking load
P_u	ultimate load
P_y	yielding load
y	distance from the center of gravity of the beam to the concrete at the level of the tension steel
Δ_{cr}	deflection at cracking
Δ_u	deflection at ultimate
Δ_y	deflection at yielding
σ_f	stress level at which the detwinning finishes
σ_s	stress level at which the detwinning starts
ε_c	strain in concrete

contribute to reducing the cost of the Fe-SMA material [14]. The shape memory alloys are mainly characterized by the Shape Memory Effect (SME), which represents the ability of the material to recover the induced permanent deformations upon heating [15]. The SME occurs when the SMA material at detwinned martensite phase is heated above the activation temperature which results in more thermodynamically stable austenite phase [4]. Fig. 1 shows the SME process of the Fe-SMA material (from point 1 to 4) on the temperature-stress-strain phase diagram. The parent austenite phase (1) at a temperature above the temperature range of the martensite phase is loaded mechanically to form the detwinned martensite phase (2) in a process called the forward martensite transformation, where a single variant dominates. The detwinning process starts at a stress level called detwinning start (σ_s) and finishes at stress level called detwinning finish (σ_f) causing macroscopic permanent deformation. The martensite remains detwinned after unloading (3). In the absence of stress, and upon the application of heat above A_s (austenite start temperature), the detwinned martensite material starts to recover the permanent deformations and completely transform to the parent austenite phase (4) at A_f (austenite finish temperature) in a process called the reverse martensite transformation. When the material cools down to room temperature, the austenite phase is reserved (1). More information about the material characteristics of Fe-SMA can be found in [14,16–19].

The objective of the study presented in this paper is to investigate the performance of RC beams strengthened with NSM Fe-SMA bars under fatigue loading. The beam stiffness degradation and the loss of prestressing force during fatigue loading are investigated. The results of the fatigued beams are compared to those of another set of un-fatigued beams (strengthened and control beams). The performance of two different anchorage systems and two grouting materials are also investigated.

2. Experimental program

2.1. Testing matrix

Four beams were tested; the beams were divided into two groups, group S (static loading), and group F (Fatigue loading). Each group consisted of two beams: one beam was strengthened in flexure with an NSM Fe-SMA bar (S-SMA and F-SMA beams), and the second beam was a control un-strengthened beam (S-C and F-C beams) is shown in Table 1.

2.2. Description of the specimens

The beams were designed as under-reinforced beams according to CSA A23.3-04 [21]. Fig. 2 shows the geometric details of a typical beam, the instrumentation details, and the loading setup. The beams were instrumented with 8 Strain Gauges (SG); 3 of them were mounted on the steel reinforcements at the mid-span (1 on the compression and 2 on the tension steel), and 5 of them were mounted along the Fe-SMA

bar. Four Linear Strain Conversion transducers (LSC) were mounted at the mid-span to measure strains: two of them were placed on the top surface of the beam and two were located at the level of the tension and compression steel. Two laser transducers were used to monitor the deflection at the mid-span as is shown in Fig. 2. The shear reinforcements included 10M two-legged closed stirrups placed at a spacing of 150 mm. The beams were reinforced with two 15M bars in tension and two 10M bars in compression with a total steel cross-sectional area of 400 mm² and 200 mm², respectively. Table 2 shows the steel and concrete material properties. It is worth mentioning that the difference between the yielding strength of the S-Beams and F-Beams was due to the fact that the S-Beams were fabricated separately. The difference between the yielding strengths is 11%. This difference is accounted for when a comparison between the two groups of beams is conducted.

2.3. Fe-SMA material characteristics

Two Fe-SMA bars were used to strengthen beams S-SMA and F-SMA. The bars were smooth without any surface finish, produced by Awaji [14], were 1000 mm long and 14.3 mm in diameter. They were tested in a unidirectional tensile testing machine to determine their stress-strain behavior. Since the available strain gauges were limited to 4% strain, the Digital Image Correlation Technique (DICT) was employed to measure the strain in the Fe-SMA bar during tensile loading. The DICT system consists of a camera that takes photos of the Fe-SMA bar every 5 s, and the photos are then analyzed using MATLAB algorithm developed by [22] to calculate the strain. Solid white dots were put on the Fe-SMA bar (Fig. 3), and an algorithm was used to report the movements of these points through analyzing the photos. After that, the strain was calculated based on the relative movements of white dots on the Fe-SMA bar. The stress-strain curve of the Fe-SMA bar is shown in Fig. 3.

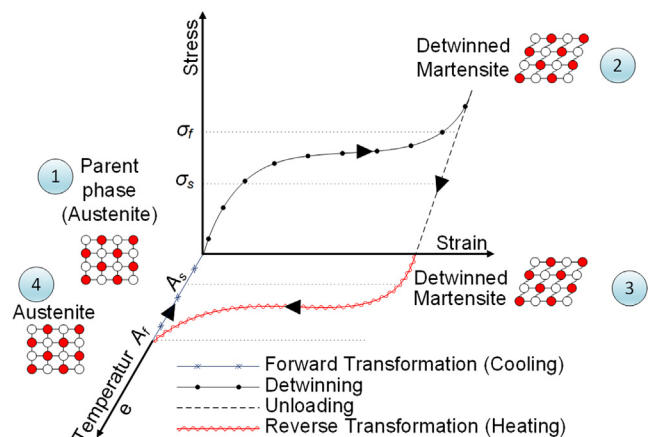


Fig. 1. The SME process of Fe-SMA material, after Lagoudas [20] and Cladera et al. [17].

Download English Version:

<https://daneshyari.com/en/article/6736810>

Download Persian Version:

<https://daneshyari.com/article/6736810>

[Daneshyari.com](https://daneshyari.com)